

## Calculation of $^{13}\text{C}$ , $^{15}\text{N}$ , and $^{29}\text{Si}$ NMR Shielding Tensors for Selected X-Substituted Silatranes Using GIAO/CSGT-SCF

Dong Hee Kim\*, Mi Jung Lee, and Se-Woung Oh†

Department of Chemistry, Kunsan National University, Kunsan 573-701, Korea

†Department of Chemistry, Mokpo National University, Muan 534-729, Korea

Received March 2, 1998

$^{13}\text{C}$ ,  $^{15}\text{N}$ , and  $^{29}\text{Si}$  NMR chemical shifts have been computed for selected X-substituted silatranes ( $\text{X}=\text{Cl}$ , F, H,  $\text{CH}_3$ ) using Gauge-Including Atomic Orbitals (GIAO) and Continuous Set of Gauge Transformations (CSGT) at the Hartree-Fock level of theory. The isotropic  $^{13}\text{C}$  chemical shifts are largely insensitive to substituent-induced structural changes. In this study, the isotropic  $^{13}\text{C}$  chemical shifts GIAO and CSGT calculations at the HF/6-31G and HF/6-31G\* levels are sufficiently accurate to aid in experimental peak assignments. The isotropic  $^{13}\text{C}$  chemical shifts X-substituted silatranes at HF/6-31G\* level are approximately 4 ppm different from the experimental values. In contrast, the isotropic  $^{15}\text{N}$  and  $^{29}\text{Si}$  chemical shifts and the chemical shielding tensors are quite sensitive to substituent-induced structural changes. These trends are consistent with those of the experiment. The  $^{15}\text{N}$  chemical shift parameters demonstrate a very clear correlation with Si-N distance, especially when we use the polarization function. Changes in anisotropy,  $\Delta\sigma$  as well as in the  $^{15}\text{N}$  isotropic chemical shifts are due primarily to changes in the value of  $\sigma_{\perp}$ . But in case of  $^{29}\text{Si}$  the correlations are not as clean as for the  $^{15}\text{N}$  chemical shift.

### Introduction

The isotropic chemical shift is an immensely useful parameter in the determination of chemical structure. This usefulness is largely due to empirical structure/chemical shift correlations. However, the problem of understanding the relationship between the chemical shift and molecular structure can be quite difficult. *Ab initio* calculations are now attainable and accurate enough to be useful in the solution of some of these problems. Especially, the calculated  $^{13}\text{C}$  chemical shifts appear to be of sufficient accuracy to aid in experimental peak assignments. A comparison of the experimental and theoretical spectra can be very useful in understanding the basic chemical shift-molecular structure relationship.

The interest in silatranes –  $\text{XSi}(\text{OCH}_2\text{CH}_2)_2\text{N}$ , 1-organyl-2,8,9-trioxa-5-aza-1-silabicyclo [3.3.3] undecanes – is due to their intriguing molecular structure, biological activity, and patterns of chemical reactivity.<sup>1-3</sup> The most intriguing aspect of this structure is the existence of and influence of a "transannular bond" between the silicon and nitrogen atoms. The transannular Si-N donor-acceptor bond (Figure 1) makes these molecules especially interesting and challenging for theoretical and experimental studies.<sup>4-12</sup>

In this study, in order to correlate the chemical shift interaction with some structure parameter we have calculated the chemical shift and the chemical shielding tensors for  $^{13}\text{C}$ ,  $^{29}\text{Si}$ , and  $^{15}\text{N}$  nuclei in X-substituted silatranes with particular attention to transannular bond using the GIAO (Gauge Including Atomic Orbitals)<sup>13</sup> and the CSGT (Continuous Set of Gauge Transformations)<sup>14</sup> methods at both Hartree-Fock levels of theory. While the GIAO method uses basis functions which depend on the field, the CSGT methods achieve gauge-invariance by accurately calculating the induced first-order electronic current density by performing a gauge transformation for each point in space.

The  $^{15}\text{N}$  and  $^{29}\text{Si}$  chemical shifts are susceptible to substituent-induced changes in the length of this transannular bond. Thus, we pay particular attention to transannular bond that effects the change of chemical shift.

### Methods of Calculation

The molecular geometries of the 1-chloro-, 1-fluoro, 1-methyl-, and 1-hydrogen silatranes were fully optimized by the Hartree-Fock (HF) method using analytical gradient techniques within the program GAUSSIAN 94.<sup>15</sup> All the geometries reported here were obtained by using the 3-21G, 6-31G, and 6-31G\* basis sets. No symmetry constraints were imposed during the geometry optimizations. Chemical shielding calculations were done with the optimized molecular geometries. In all calculations, 3-21G, 6-31G, and 6-31G\* basis sets were employed on all atoms. The GIAO and CSGT methods were also implemented into GAUSSIAN 94 for the calculation of the isotropic  $^{13}\text{C}$ ,  $^{29}\text{Si}$  and  $^{15}\text{N}$  NMR shifts and their nuclear shielding constants for silatranes.

The chemical shift  $\delta$  is obtained from  $\sigma$  by

$$\delta = \sigma_{\text{ref}} - \sigma$$

where  $\sigma_{\text{ref}}$  is the shielding tensor of the reference compound, in our case, TMS for  $^{13}\text{C}$ . A negative value of  $\delta$  means a stronger shielding in the silatranes than in TMS (equivalent to an upfield or low-frequency shift), while a positive value of  $\delta$  means less shielding than in TMS. The chemical shielding convention used in the *ab initio* calculations is the  $\sigma$  scale, in which algebraically larger numbers indicate higher shielding, opposite in sense to the  $\delta$  scale of chemical shifts.

### Results and Discussion

This study is the continuation of our previous studies,

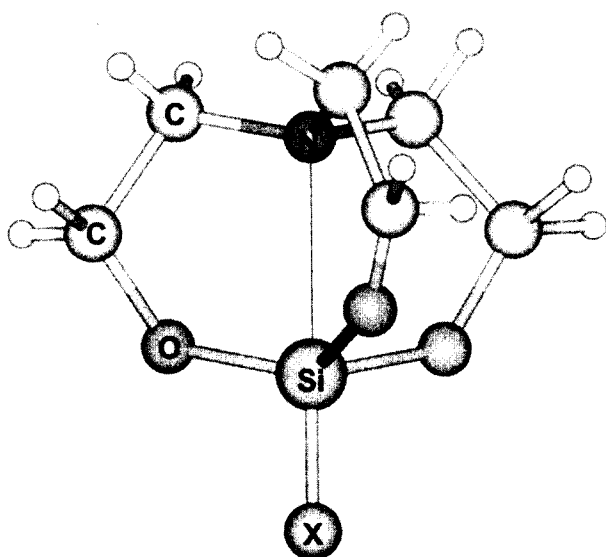


**Figure 1.** The Structure of X-Substituted Silatrane (X=Cl, F, H, CH<sub>3</sub>).

which have reported <sup>13</sup>C, <sup>15</sup>N, and <sup>29</sup>Si NMR chemical shifts computed for selected X-substituted silatranes using GIAO method at the small basis sets.<sup>16</sup> In this study, we added CSGT method and polarization functions to previous study for calculation of chemical shielding tensors and isotropic chemical shifts of <sup>13</sup>C, <sup>29</sup>Si, and <sup>15</sup>N in the set of some substituent silatranes.

The structural parameters of X-substituted silatranes and the isotropic <sup>13</sup>C chemical shifts are tabulated in Tables 1 and 2, respectively. Experimentally, the OCH<sub>2</sub> carbons of the silatranes framework have isotropic chemical shifts in the neighborhood of 58 ppm and the NCH<sub>2</sub> carbons have isotropic chemical shifts of approximately 51 ppm, as

**Table 1.** The Geometrical Parameters of Selected X-Substituted Silatranes

X	Basis Set	Distance (pm)		Energy(a.u)
		r <sub>Si-N</sub>	r <sub>Si-X</sub>	
Cl	3-21G	222.94	217.03	-1255.2908
	6-31G	248.25	214.42	-1261.4883
	6-31G*	257.46	205.75	-1261.8055
	<sup>a</sup> X-Ray	202.30		
F	3-21G	239.14	161.48	-896.9190
	6-31G	249.07	165.26	-901.4556
	6-31G*	255.49	158.10	-901.7817
	<sup>b</sup> ED	232.40	156.80	
H	<sup>c</sup> X-Ray	204.20	162.20	
	3-21G	249.63	146.11	-798.5078
	6-31G	264.47	146.49	-802.5554
	6-31G*	265.56	145.94	-802.8423
CH <sub>3</sub>	3-21G	263.33	187.05	-837.3579
	6-31G	273.92	186.83	-841.5992
	6-31G*	274.10	186.06	-841.8930
	<sup>d</sup> ED	245.35	185.30	
	<sup>e</sup> X-Ray	217.54	187.00	

The experimental values taken from refs. 5-9 (<sup>a</sup> Reference 5. <sup>b</sup> Reference 6. <sup>c</sup> Reference 7. <sup>d</sup> Reference 8. <sup>e</sup> Reference 9.)

shown in Table 2. These assignments and the peak assignments for the substituents bound to the silicon atom are based upon solution-state <sup>13</sup>C NMR studies<sup>17,18</sup> and variable-field high-resolution solid-state <sup>13</sup>C NMR results.<sup>19</sup> Also, all of calculated isotropic chemical shifts for the OCH<sub>2</sub> carbons of the silatranes framework are larger than those of NCH<sub>2</sub>. Their assignment, therefore, was verified by calculated isotropic <sup>13</sup>C chemical shifts, although there were some assignment problems for the <sup>13</sup>C spectra in both the solution and solid NMR experiments.

As with reported solution-state <sup>13</sup>C NMR studies,<sup>17,18</sup> the isotropic <sup>13</sup>C chemical shift of silatranes in the solid-state<sup>19</sup> appears to be nearly independent of the Si-N distances (or substituents). Also the calculated isotropic <sup>13</sup>C chemical shift of silatranes appears to be nearly independent of the Si-N distance. One should expect that the isotropic <sup>13</sup>C chemical shift of silatranes calculated using 6-31G\* will be improved more than that of 6-31G basis set because they are especially strongly correlated molecules composed of electronegative atoms. In the CSGT method, the isotropic <sup>13</sup>C chemical shifts calculated at 6-31G\* level of theory are improved about 3 ppm more than those of 6-31G while there are only a little difference in GIAO-SCF calculation. Both of the results using GIAO and CSGT methods at HF/6-31G\* level are about 4 ppm different from the experimental values as shown in Table 2. It is well-known that the shielding tensor is very sensitive to the quality and size of the

**Table 2.** Comparison of Calculated and Experimental Isotropic <sup>13</sup>C Chemical Shifts of Selected X-Substituted Silatranes

X	Basis Set	Method	OCH <sub>2</sub>	NCH <sub>2</sub>	α
Cl	3-21G	GIAO	50.07	45.08	
		CSGT	43.14	37.31	
	6-31G	GIAO	55.42	48.07	
		CSGT	52.91	44.66	
	6-31G*	GIAO	55.07	48.32	
		CSGT	55.17	47.52	
	Exp		60.10	52.70	
F	3-21G	GIAO	50.60	46.47	
		CSGT	43.92	38.62	
	6-31G	GIAO	54.85	48.61	
		CSGT	52.60	45.41	
	6-31G*	GIAO	54.72	48.63	
		CSGT	54.99	47.94	
	Exp		58.50	51.40	
H	3-21G	GIAO	50.17	44.69	
		CSGT	44.26	37.06	
	6-31G	GIAO	54.61	47.69	
		CSGT	52.94	44.44	
	6-31G*	GIAO	54.42	48.26	
		CSGT	54.44	47.69	
	Exp		58.20	51.80	
CH <sub>3</sub>	3-21G	GIAO	51.56	45.35	-0.67
		CSGT	45.17	37.62	-2.00
	6-31G	GIAO	55.29	47.78	-1.32
		CSGT	53.12	44.45	-0.15
	6-31G*	GIAO	54.86	48.33	-1.12
		CSGT	55.24	47.70	0.82
	Exp		58.40	49.20	3.80

<sup>a</sup> All Shifts are taken relative to TMS.

**Table 3.** The Absolute  $^{15}\text{N}$  NMR Shift Parameters of Selected X-Substituted Silatranes Using GIAO

X	Basis Set	$\sigma_{\parallel}$	$\sigma_{\perp}$	$\Delta\sigma$	$\sigma_{\text{iso}}$
Cl	3-21G	239.23	279.82	-40.59	266.29
	6-31G	226.29	287.52	-61.23	267.11
	6-31G*	223.47	293.56	-70.09	270.20
F	3-21G	236.03	287.93	-51.90	270.63
	6-31G	225.71	287.76	-62.05	267.08
	6-31G*	223.26	292.14	-68.88	269.18
H	3-21G	234.52	298.24	-63.72	277.00
	6-31G	223.56	302.02	-78.46	275.87
	6-31G*	221.94	300.96	-79.02	274.62
$\text{CH}_3$	3-21G	233.24	303.74	-70.50	280.24
	6-31G	222.93	306.28	-83.35	278.49
	6-31G*	221.27	305.53	-84.26	277.44

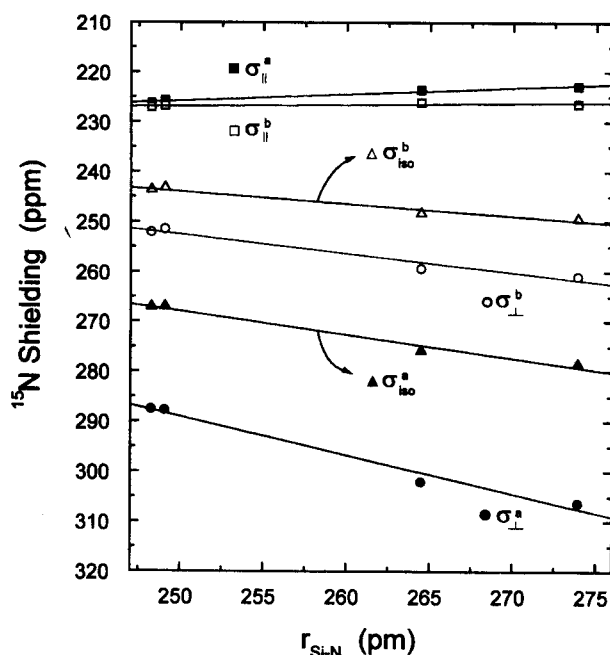
basis set used.<sup>20,21</sup> Thus, to make a comparison with the experimental values precisely, we need to use larger basis sets or the other theory<sup>22,23</sup> to describe electron correlation effect because all of carbon atoms are bound to electronegative atoms, e.g., oxygen or nitrogen atom.

In contrast to the isotropic  $^{13}\text{C}$  chemical shift, the isotropic  $^{15}\text{N}$  chemical shift demonstrates a very clear correlation with Si-N distance. The  $^{15}\text{N}$  NMR shielding tensors of selected X-substituted silatranes, as well as the isotropic  $^{15}\text{N}$  chemical shifts, by GIAO-SCF and CSGT-SCF calculation at the Hatree Fock levels are given in Tables 3 and 4. Close inspection of Tables 3 and 4 reveal the isotropic  $^{15}\text{N}$  chemical shift and chemical shielding tensors indeed exhibit modest dependencies on substituent variation. The effect of the substituent on the structure of a silatrane is perhaps most directly seen in Si-N distance. More electronegative substituents give a silatrane geometry with a smaller Si-N distance than those characteristic of silatranes with less electronegative substituents. We can see clearly the trend in Figures 2 and 3. For the set of silatranes in this study, we can see from Tables 3 and 4 that, as the Si-N distance decreases, the absolute isotropic  $^{15}\text{N}$  chemical shift decreases, with changes about 7 ppm in both of methods. The larger absolute calculated value means higher shielding. This trend is consistent with that of experiments.<sup>19,24</sup>

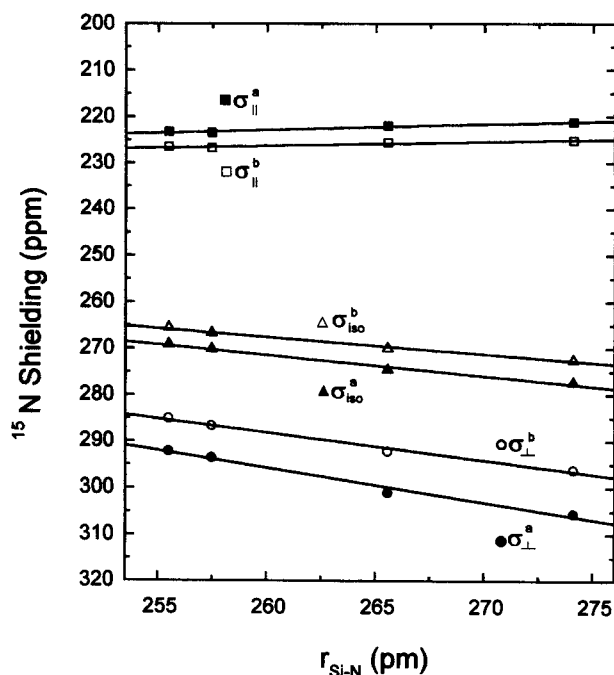
Since the isotropic shielding, usually observed in the li-

**Table 4.** The Absolute  $^{15}\text{N}$  NMR Shift Parameters of Selected X-Substituted Silatranes Using CSGT

X	Basis Set	$\sigma_{\parallel}$	$\sigma_{\perp}$	$\Delta\sigma$	$\sigma_{\text{iso}}$
Cl	3-21G	230.18	243.63	-13.45	239.15
	6-31G	227.06	252.11	-25.05	243.76
	6-31G*	226.73	286.70	-59.97	266.71
F	3-21G	228.04	245.35	-17.31	239.58
	6-31G	226.77	251.49	-24.72	243.25
	6-31G*	226.51	285.10	-58.59	265.57
H	3-21G	227.53	251.36	-23.83	243.41
	6-31G	226.13	259.38	-33.25	248.30
	6-31G*	225.57	292.20	-66.63	269.99
$\text{CH}_3$	3-21G	227.26	252.78	-25.52	244.27
	6-31G	226.41	260.93	-34.52	249.43
	6-31G*	225.16	296.14	-70.98	272.48

**Figure 2.** Correlation curves for some  $^{15}\text{N}$  chemical shift parameters vs  $r_{\text{Si-N}}$ . All of data were calculated using <sup>a</sup>GIAO and <sup>b</sup>CSGT at the HF/6-31G level.

quid state, is simply the mean of the component of the  $^{15}\text{N}$  chemical shift tensor,  $\sigma_{\text{iso}} = 1/3(\sigma_{xx} + \sigma_{yy} + \sigma_{zz})$ , other combinations or chemical shielding tensors, might be expected to follow different trends. The shielding anisotropy, i.e., the individual tensor components of the shielding tensor, should be even more sensitive to the quality of the quantum-chem-

**Figure 3.** Correlation curves for some  $^{15}\text{N}$  chemical shift parameters vs  $r_{\text{Si-N}}$ . All of data were calculated using <sup>a</sup>GIAO and <sup>b</sup>CSGT at the HF/6-31G\* level.

**Table 5.** The Absolute  $^{29}\text{Si}$  NMR Shift Parameters of Selected X-Substituted Silatranes Using GIAO

X	Basis Set	$\sigma_{\parallel}$	$\sigma_{\perp}$	$\Delta\sigma$	$\sigma_{\text{iso}}$
Cl	3-21G	541.51	564.98	-23.47	557.16
	6-31G	503.02	509.92	-6.90	507.62
	6-31G*	496.44	502.95	-6.51	500.78
F	3-21G	567.15	608.83	-41.68	594.93
	6-31G	518.15	550.92	-32.77	540.00
	6-31G*	510.46	533.61	-23.15	525.90
H	3-21G	558.92	567.60	-8.68	564.70
	6-31G	521.11	516.62	4.49	518.12
	6-31G*	504.33	502.04	2.29	502.80
$\text{CH}_3$	3-21G	586.67	554.37	32.30	565.14
	6-31G	538.28	479.54	58.74	499.12
	6-31G*	517.97	470.12	47.85	486.07

**Table 6.** The Absolute  $^{29}\text{Si}$  NMR Shift Parameters of Selected X-Substituted Silatranes Using CSGT

X	Basis Set	$\sigma_{\parallel}$	$\sigma_{\perp}$	$\Delta\sigma$	$\sigma_{\text{iso}}$
Cl	3-21G	402.24	526.00	-123.76	484.75
	6-31G	400.13	459.73	-59.6	439.86
	6-31G*	436.11	445.23	-9.12	442.19
F	3-21G	432.08	496.44	-64.36	474.99
	6-31G	418.49	481.37	-62.88	460.41
	6-31G*	449.21	498.45	-49.24	482.04
H	3-21G	434.76	524.97	-90.21	494.90
	6-31G	429.88	472.69	-42.81	458.42
	6-31G*	444.01	459.36	-15.35	454.25
$\text{CH}_3$	3-21G	449.04	478.81	-29.77	468.89
	6-31G	447.14	427.90	19.24	434.32
	6-31G*	458.74	420.04	38.73	432.94

ical method used than the isotropic shielding constant. Here, we define the shielding anisotropy  $\Delta\sigma$  as the difference between the parallel and the orthogonal principal components:<sup>21</sup> ( $\Delta\sigma = \sigma_{\parallel} - \sigma_{\perp}$ ). The  $\sigma_{\parallel}$  element lies along the silicon-nitrogen internuclear axis and the  $\sigma_{\perp}$  elements lie in a plane perpendicular to the silicon-nitrogen internuclear axis. Figures 2 and 3 graphically depict the plots of the various  $^{15}\text{N}$  chemical shift parameters ( $\sigma_{\text{iso}}$ ,  $\sigma_{\parallel}$ ,  $\sigma_{\perp}$ ) versus Si-N distance. Particularly, we recognize a very clear correlation for  $\sigma_{\text{iso}}$ ,  $\sigma_{\perp}$ ,  $\sigma_{\parallel}$  in Figure 3 which is the calculated result using polarization function. As the Si-N distance decreases, the absolute chemical shielding anisotropy by the GIAO-SCF/6-31G\* level changes in magnitude, from -84.26 to -70.09 ppm for the ethyl and chloro derivatives, respectively. Changes in  $\Delta\sigma$  as well as in the  $^{15}\text{N}$  isotropic chemical shifts are due primarily to changes in the value of  $\sigma_{\perp}$ , which varies between 305.53 and 293.56 ppm at the GIAO-SCF/6-31G\* level, while it varies between 296.14 and 286.70 ppm at the CSGT-SCF/6-31G\* level. Because of the z-symmetry of the Si-N interaction, the value of  $\sigma_{\parallel}$  is being fairly constant and exhibiting no easily recognized dependence on substituent.

The chemical shielding tensor for  $^{29}\text{Si}$  yields a more striking dependence on the substituent variation than that for  $^{15}\text{N}$  because the substituent is directly attached to silicon. Although the correlations are not as clean as for the  $^{15}\text{N}$  chem-

ical shift, the calculated variation in the  $^{29}\text{Si}$  chemical shift is much larger. The principal elements of the  $^{29}\text{Si}$  chemical shielding tensors, as well as the isotropic chemical shifts, are given in Tables 5 and 6. The  $^{29}\text{Si}$  isotropic chemical shifts and anisotropies calculated by GIAO-SCF and CSGT-SCF methods exhibit wider variation than do those of the  $^{15}\text{N}$ . For  $^{29}\text{Si}$  the anisotropy varies from -6.51 to 47.85 ppm for the chloro and methyl derivatives, respectively, with all of the principal elements exhibiting a dependence on the substituent at the GIAO-SCF/6-31G\* level, while it varies from -9.12 to 38.73 ppm at the CSGT-SCF/6-31G\* level.  $\sigma_{\perp}$  changes by approximately 32 ppm with increasing Si-N distance, and  $\sigma_{\parallel}$  changes by approximately 22 ppm while the variation of  $\sigma_{\parallel}$  for  $^{15}\text{N}$  is nearly constant as mentioned above.

The correlations are not also as clear as those discussed above for the  $^{15}\text{N}$  data. The added complication is the presence and the local effect of the directly-attached substituent. Thus, the substituent effect on the  $^{29}\text{Si}$  chemical shift can be viewed as having three types of origins: i) the geometry-structure effect associated with variations in the  $\angle\text{OSiO}$  bond angle; ii) the substituent effect due to variations in the N-Si transannular interaction; and iii) the direct substituent effect. This third type of effect is, of course, absent in the  $^{15}\text{N}$  case, so one can expect that the interpretation of chemical shift data in terms of the transannular bond should be more difficult for  $^{29}\text{Si}$  than for  $^{15}\text{N}$ . In addition, 1-chloro- and 1-fluorosilatranes are strongly correlated molecules that have electronegative atoms attached directly to silicon. 1-chloro and 1-fluorosilatrane are strongly correlated molecules composed of electronegative atoms as mentioned previously. In order to interpret for this effect on nmr parameters, we need to adopt larger basis sets than those in this study because the shielding tensor is very sensitive to the quality and size of the basis set used<sup>20,21</sup> or the other theory,<sup>22,23</sup> e.g., GIAO-MP2 and DFT theories as mentioned for  $^{13}\text{C}$  above.

In conclusion, the isotropic  $^{13}\text{C}$  chemical shift of silatranes in these calculations appears to be nearly independent of the Si-N distances (or substituents). In contrast to the isotropic  $^{13}\text{C}$  chemical shift, the  $^{15}\text{N}$  chemical shift demonstrates a very clear correlation with Si-N distance. For  $^{29}\text{Si}$ , correlation between nmr parameters and Si-N distance is not as simple to interpret as for the  $^{15}\text{N}$  results because the  $^{29}\text{Si}$  chemical shift tensor is strongly affected by the directly attached substituent as well as by the silicon-nitrogen transannular interaction. To predict quantitatively the effects of substituent variation on  $^{29}\text{Si}$  nmr chemical shift, we need to perform higher-quality calculation than Hartree-Fock level.

## References

1. Voronkov, M. G. *Pure Appl. Chem.* **1966**, 13, 35.
2. Voronkov, M. G.; Dyakov, V. M.; Kirpichenko, S. V. *J. Organomet. Chem.* **1982**, 233, 1.
3. Hencsei, P.; Parkanyi, L. *Rev. Silicon, Germanium, Tin Lead Compd.* **1985**, 8, 191.
4. (a) Csonka, G. I.; Hencsei, P. *J. Comput. Chem.* **1994**, 15, 385. (b) Csonka, G. I.; Hencsei, P. *J. Comput. Chem.* **1996**, 17, 767.
5. Kemme, A. A.; Bleidelis, Ya.; Pestunovich, V. A.; Bar-

- yshok, V. P.; Voronkov, M. G. *Dokl. Akad. Nauk SSSR* **1978**, 243, 688.
6. Forgacs, G.; Kolonits, M.; Hargittai, I. *Struct. Chem.* **1990**, 1, 245.
  7. Parkanyi, L.; Hencsei, P.; Bihatsi, L.; Müller, T. J. *Organomet. Chem.* **1984**, 1, 269.
  8. Shen, Q.; Hilderbrandt, R. L. *J. Mol. Struct.* **1980**, 64, 257.
  9. Parkanyi, L.; Bihatsi, L.; Hencsei, P. *Cryst. Struct. Commun.* **1978**, 7, 435.
  10. Pauling, L. *The Nature of the Chemical Bond*, Cornell University Press: Ithaca, NY, 1960.
  11. Glidewell, C. *Inorg. Chim. Acta*, **1976**, 20, 113.
  12. Sidurkin, V. F.; Balakchi, G. K.; Voronkov, M. G.; Pestunovich, V. A. *Dokl. Akad. Nauk SSSR* **1988**, 301, 1235.
  13. Ditchfield, R. *Mol. Phys.* **1974**, 27, 789.
  14. Keith, T. A.; Bader, R. F. W. *Chem. Phys. Lett.* **1993**, 210, 223.
  15. Frisch, M. J.; Trucks, G. W.; Schlegel, G. B.; Gill, P. M. W.; Johnson, B. G.; Robb, M. A.; Cheeseman, J. R.; Keith, T.; Petersson, G. A.; Montgomery, J. A.; Raghavachari, K.; Al-Lagam, M. A.; Zakrzewski, V. G.; Ortiz, J. V.; Foresman, J. B.; Cioslowski, J.; Stefanov, B. B.; Nanayakkara, A.; Challacombe, M.; Peng, C. Y.; Ayala, P. Y.; Chen, W.; Wong, M. W.; Andres, J. L.; Replogle, E. S.; Gomperts, R.; Martin, R. L.; Fox, D. J.; Binkley, J. S.; Defrees, D. J.; Baker, J.; Stewart, J. P.; Head-Gordon, M.; Gonzalez, C.; Pople, J. A. Gaussian 94, Gaussian Inc.: Pittsburgh, Pa. 1995.
  16. Kim, D. H.; Lee, M. J. *Bull. Korean Chem. Soc.* **1997**, 18, 981.
  17. Bellama, J. M.; Nice, J. D.; Ben-Zvi, N. *Magn. Reson. Chem.* **1986**, 24, 748.
  18. Harris, R. K.; Jones, J.; Ng, S. J. *Magn. Reson.* **1978**, 30, 521.
  19. Iwamiya, J. H.; Maciel, G. E. *J. Am. Chem. Soc.* **1993**, 115, 6835.
  20. Fukui, H. *Magn. Res. Rev.* **1987**, 11, 205.
  21. Chesnut, D. B. In *Annual Reports on NMR Spectroscopy*; Webb, G. A., Ed; Academic Press: New York, 1989; Vol. 21.
  22. (a) Gauss, J. J. *Chem. Phys.* **1993**, 99, 3629. (b) Olah, G. A.; Rasul, G.; Heiliger, L.; Prakash, G. K. S. *J. Am. Chem. Soc.* **1996**, 118, 3580.
  23. (a) Rauhut, G.; Puyear, K. W.; Pulay, P. *J. Phys. Chem.* **1996**, 100, 6310. (b) Schreckenbach, G.; Ziegler, T. *J. Phys. Chem.* **1995**, 99, 606.
  24. Pestunovich, V. A.; Shterenberg, B. Z.; Lippmaa, E. T.; Myagi, M. Ya.; Alla, M. A.; Tandura, S. N.; Baryshok, V. P.; Petukhov, L. P.; Voronkov, M. G. *Dokl. Akad. Nauk SSSR* **1981**, 258, 1410.

## Synthesis of Highly Crosslinked Temperature-resistant Poly(vinyl ethers) by Free Radical Polymerization

Ju-Yeon Lee\* and Ji-Hyang Kim

Department of Chemistry, Inje University, 607 Aebang-dong, Kimhae 621-749, Korea

Received April 10, 1998

2,4-Di-(2-vinyloxyethoxy)benzylidenemalononitrile (**2a**), methyl 2,4-di-(2-vinyloxyethoxy)benzylidenecyanoacetate (**2b**), 3,4-di-(2-vinyloxyethoxy)benzylidenemalononitrile (**4a**), and methyl 3,4-di-(2-vinyloxyethoxy)benzylidenecyanoacetate (**4b**), 2,5-di-(2-vinyloxyethoxy)benzylidenemalononitrile (**6a**), and methyl 2,5-di-(2-vinyloxyethoxy)benzylidenecyanoacetate (**6b**) were prepared by the condensation of 2,4-di-(2-vinyloxyethoxy)benzaldehyde (**1**), 3,4-di-(2-vinyloxyethoxy)benzaldehyde (**3**), and 2,5-di-(2-vinyloxyethoxy)benzaldehyde (**5**) with malononitrile or methyl cyanoacetate, respectively. Trifunctional divinyl ether monomers **2**, **4** and **6** were polymerized readily by free radical initiators to give optically transparent swelling poly(vinyl ethers) **7-9**. Polymers **7-9** were not soluble in common organic solvents such as acetone and DMSO due to crosslinking. Polymer **7-9** showed a thermal stability up to 300 °C in TGA thermograms.

### Introduction

Electron-rich alkyl vinyl ethers do not radically homopolymerize, but copolymerize readily with electron-poor olefins such as vinylidene cyanide,<sup>1</sup> 2-vinylcyclopropane-1,1-dicarbonitrile,<sup>2</sup> alkyl acrylate,<sup>3-5</sup> alkyl vinyl ketone,<sup>6</sup> maleic anhydride,<sup>7,8</sup> and others by radical initiators. These facile reactions proceed through an electron donor-acceptor (EDA) complex, which generates zwitterion or diradical tetramethylenes as initiating species.<sup>9-12</sup> Trisubstituted elec-

tron-poor olefins such as benzylidenemalononitrile and ethyl benzylidenecyanoacetate do not homopolymerize, but copolymerize with ethyl acetate, styrene, acrylonitrile, or methyl acrylate by radical initiators.<sup>13-19</sup> The captodative (cd) olefins with geminal electron-withdrawing and electron-donating groups have a strong tendency to polymerize due to the resonance stabilization of propagating radical species, if appropriate electron-donor and -acceptor combinations in the cd substituents are chosen.<sup>20,21</sup> Bifunctional monomers containing both electron-rich alkyl vinyl ether group and